# A DNA Biosensor Based Interface States of a Metal–Insulator–Semiconductor Diode for Biotechnology Applications

A.A. Al-Ghamdi[a], O.A. Al-Hartomy[a,b], R. Gupta[c], F. El-Tantawy[d], E. Taskan[e], H. Hasar[e] and F. Yakuphanoglu[f,*]

[a]Department of Physics, Faculty of Science, King Abdulaziz University, Jeddah, Saudi Arabia

[b]Department of Physics, Faculty of Science, Tabuk University, Tabuk 71491, Saudi Arabia

[c]Engineering Research Center, North Carolina A & T State University, Greensboro, North Carolina 27411, USA

[d]Department of Physics, Faculty of Science, Suez Canal University, Ismailia, Egypt

[e]Department of Environmental Engineering, Firat University, Elaziğ, Turkey

Center for Biotechnology Research, Firat University, Elazig, Turkey

[f]Department of Physics, Faculty of Science, Firat University, Elazig, Turkey

*(Received June 21, 2011; revised version December 2011; in final form January 2, 2012)*

We studied how a DNA sensor based on the interface states of a conventional metal–insulator–semiconductor diode can be prepared for biotechnology applications. For this purpose, the $p$-type silicon/metal diodes were prepared using $SiO_2$ and DNA layers. The obtained results were analyzed and compared with interfaces of DNA and $SiO_2$. It is seen that the ideality factor (1.82) of the Al/$p$-Si/$SiO_2$/DNA/Ag diode is lower than that (3.31) of the Al/$p$-Si/$SiO_2$/Ag diode. This indicates that the electronic performance of DNA/Si junction was better than that of $SiO_2$/Si junction. The interface states of the Al/$p$-Si/$SiO_2$/DNA/Ag and Al/$p$-Si/$SiO_2$/Ag junctions were analyzed by conductance technique. The obtained $D_{it}$ values indicate that the DNA layer is an effective parameter to control the interface states of the conventional Si based on metal/semiconductor contacts. Results exhibited that DNA based metal–insulator–semiconductor diode could be used as DNA sensor for biotechnology applications.

PACS: 73.40.Jn, 81.05.Fb, 73.30.+y

## 1. Introduction

The metal/semiconductor (MS) contacts are of great importance for the potential use in electronic and optoelectronic devices [1–4] and MS diodes have been studied by many researchers using various organic semiconducting materials [5–8]. It is well known that the electrical characteristics of metal/semiconductor contacts are controlled mainly by their surface properties [8–11]. An MS diode possesses a thin interfacial native oxide layer, which has a big influence on electrical characteristics of diode [10]. The electrical properties of MS diode can be controlled by adsorption of small organic compound on the inorganic semiconductor surface. The deoxyribonucleic acid (DNA), which is central to every living organism, is a subject of interest for its physical properties, and particularly for a great potential of application in photonics and molecular electronics [12]. DNA can be synthesized artificially and extracted from living organisms in its purity. It is the most stable molecule even under high temperature conditions (90 °C) [13].

DNA device with metal/semiconductor contacts are still rare [14–16]. In recent years, there are some studies on the electrical conduction of the DNA molecules which reveal that they may act as either semiconductor with nanosize dimensions or non-semiconductor materials (i.e., insulator or metal) [17–19].

In our previous study, we have fabricated a Al/$p$-Si/DNA/Ag diode for optical sensor applications, in which we have used DNA of band 15 at all microbial fuel cell (MFC) samples detected as *Shewanella halitotis* [20].

In present study, we have used DNA of band 18 at all microbial fuel cell (MFC) samples detected as *Enterococcus sp.* and $SiO_2$ layer to fabricate a Al/$p$-Si/$SiO_2$/DNA/Ag diode. To best of our knowledge, no study on Al/$p$-Si/$SiO_2$/DNA/Ag diode has been reported. The aim of this study is to fabricate a DNA based MS diode for electronic device applications. DNA purified from an MFC operating in the environmental biotechnology area was used to develop the biosensor. The current–voltage and capacitance–voltage measurements were performed to analyze the electrical properties of the DNA based MS diode.

## 2. Experimental details

### 2.1. DNA protocol description

Total DNA was extracted from the MFC, which produces directly the electricity energy while treating wastewater, at different time intervals to reveal the changes in the microbial communities over time using denaturing gradient gel electrophoresis (DGGE) analysis. DNA was extracted with PowerSoil DNA isolation kit according to manufacturer's instructions. Extracted DNA samples were stored at −20 °C. The crude DNA sample including a mixed culture was used as a template

* corresponding author; e-mail: fyhanoglu@firat.edu.tr

for the polymerase chain reaction (PCR). Fragments corresponding to nucleotide positions 341–534 of the *Escherichia coli* 16S rRNA gene sequence were amplified with the forward primer GC-BacV3f (5-CCT ACG GGA GGC AGC AG-3) to which at the 5′ end a GC clamp was added to stabilize the melting behavior of the DNA fragments in the DGGE, and the reverse primer 534r (5′ — ATT ACC GCG GCT GCT GG-3′) [21]. PCR amplification was performed using Thermocycler TECHNE/TC-512 with the following program: initial denaturation at 95 °C for 5 min followed by 30 cycles of denaturation at 94 °C for 30 s, primer annealing at 50 °C for 1 min and primer extension at 72 °C for 2 min, and final extension at 72 °C for 10 min.

The presence of PCR products was confirmed by 1% (w/v) agarose gel electrophoresis and staining with ethidium bromide prior to DGGE analysis. DGGE was performed with the INGENY phor U-2, Ingeny International BV. PCR samples were loaded onto 8% (w/v) polyacrylamide gel (acrylamide/bisacrylamide (37.5:1) stock solution, Bio–Rad) in TAE (40 mM Tris, 20 mM acetic acid, 1 mM EDTA, pH 8.3) with denaturing gradient ranging from 35% to 60% (100% denaturant contains 7 M urea and 40% formamide). The electrophoresis was run at 60 °C with 100 V for 18 h.

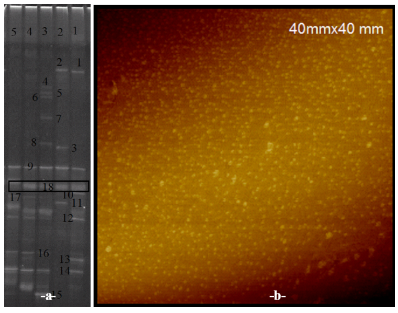


Fig. 1. (a) DGGE bands for five MFC conditions, (b) AFM image of the DNA thin film deposited on the $SiO_2$/Si.

After electrophoresis, the gel was stained in a SYBR gold solution (100 mL/L in TAE) for 35 min and photographed by a Gel Monitoring System (Vilberlourmat), as seen in Fig. 1a. Bands in DGGE gels were excised with a razor blade and placed in sterile 1 ml vials. DNA was eluted into 20 mL of water and frozen at −20 °C. The eluted DNA was used as template in PCR reactions with the primers BacV3f (without GC clamp) and 534r using the same PCR programs described above. The sequencing of the purified products was performed at DNA Sequencing Facility, IONTEK firm, Turkey. DGGE of 16S rRNA genes was applied to reveal successive changes in the microbial communities of the MFC (Fig. 1a). In the DGGE analysis, 18 bands were numbered at different operating conditions. Band 18 at all MFC samples was detected as *Enterococcus sp.* (Accession No. AY489118.1), which means dominant microorganism in MFC.

### *2.2. Fabrication of the diodes*

For fabrication of the $p$-Si/$SiO_2$ [20] and $p$-Si/$SiO_2$/DNA diodes, a $p$-Si wafer was firstly chemically cleaned using the RCA cleaning procedure. After surface cleaning, the Al metal was evaporated onto $p$-Si substrate using a PVD-HANDY/2S-TE (Vaksis Company) vacuum thermal evaporation. The native oxide on $p$-Si layer was removed in HF+$10H_2O$ solution and then was rinsed in deionized water using an ultrasonic bath for 10–15 min and finally was chemically cleaned according to method based on successive baths of methanol and acetone. The Si substrates were used for the preparation of the diodes. One of them was oxidized at room temperature for 2 days. Then, the DNA film was carefully placed by deposition of 10 $\mu$ L DNA solution on the $p$-Si wafer by spin coating technique and slowly spread on top of it and then, it was dried at room temperature for 12 h. The thickness of the DNA film was obtained to be $360 \pm 2.5$ nm. The Schottky contact was formed by Ag paint on the DNA organic layer. The prepared diodes are Al/$p$-Si/$SiO_2$/DNA/Ag and Al/$p$-Si/$SiO_2$/Ag [20] junctions. The diode contact area was calculated to be $3.14 \times 10^{-2}$ cm$^2$. The current–voltage ($I$–$V$) and capacitance–voltage ($C$–$V$) characteristics of the Al/$p$-Si/$SiO_2$/DNA/Ag and Al/$p$-Si/$SiO_2$/Ag junctions were measured with Keithley 4200 semiconductor characterization system.

## 3. Results and discussion

### *3.1. Structural properties and electrical characteristics*

The AFM image of the DNA thin film deposited on the $SiO_2$/Si is shown in Fig. 1b. As seen in Fig. 1b, the DNA molecules are formed from the clusters. The roughness of the film was determined to be 26.9 nm.

In our previous study, we have fabricated an Al/$p$-Si/Ag junction and we have analyzed its electrical characterization by $I$–$V$ and $C$–$V$ measurements [20]. The obtained results indicated that the ideality factor of the Al/$p$-Si/Ag diode is higher than unity. Thus, in present study, we evaluated that Al/$p$-Si/Ag diode has a metal–oxide–semiconductor structure as Al/$p$-Si/$SiO_2$/Ag. The electrical characteristics of Al/$p$-Si/Ag diode (hereinafter "Al/$p$-Si/$SiO_2$/Ag diode") were used to explain the effect of *Enterococcus sp.* DNA layer on the electrical parameters of the Al/$p$-Si/Ag diode.

The current–voltage characteristics of the Al/$p$-Si/$SiO_2$/DNA/Ag and Al/$p$-Si/$SiO_2$/Ag [20] junctions are shown in Fig. 2. The junctions exhibit a good rectifying behavior and the rectifying behavior of the Al/$p$-Si/$SiO_2$/Ag diode changes with DNA modification. The current–voltage characteristics of the Al/$p$-Si/$SiO_2$/DNA/Ag and Al/$p$-Si/$SiO_2$/Ag junctions can be analyzed by the following relation [22]:

$$I = AA^*T^2 \exp\left(\frac{q\phi_{\text{eff}}}{kT}\right)\left[\exp\left(\frac{q(V - IR_s)}{nkT}\right)\right], \qquad (1)$$

where $A^*$ is the Richardson constant with a value of

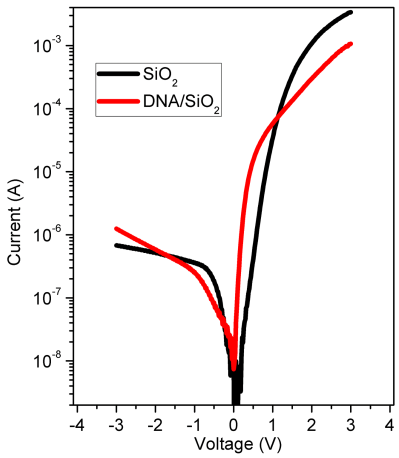


Fig. 2. Current–voltage characteristics of the Al/*p*-Si/$SiO_2$/DNA/Ag and Al/*p*-Si/$SiO_2$/Ag [20] junctions.

32 A $cm^{-2}K^{-2}$ for *p*-type silicon, $R_s$ is the series resistance, $V$ is the applied voltage, $n$ is the ideality factor, $k$ is the Boltzmann constant, $T$ is the temperature and $\phi_{eff}$ is the effective barrier given by [23, 24]:

$$q\phi_{eff} = q\phi_b + kT\beta l, \tag{2}$$

where $\beta$ is the structure-dependent attenuation factor that depends on the tunneling mechanism, $l$ is the film thickness of DNA film and the second term in Eq. (2) contributes to the effective barrier height of the interfacial layer.

As seen in Fig. 2, the $I$–$V$ characteristics of the diode are linear at lower forward voltages. The ideality factors of the Al/*p*-Si/$SiO_2$/DNA/Ag and Al/*p*-Si/$SiO_2$/Ag junctions were obtained to be $1.82 \pm 0.15$ and $3.31 \pm 0.11$, respectively. The ideality factor of the Al/*p*-Si/$SiO_2$/DNA/Ag diode is lower than that of the Al/*p*-Si/$SiO_2$/Ag. This indicates that the electronic performance of DNA/Si junction is changed by DNA molecules. The barrier height values of the Al/*p*-Si/$SiO_2$/DNA/Ag and Al/*p*-Si/$SiO_2$/Ag diodes were obtained to be 0.76 eV and 0.82 eV, respectively, and these values are higher than that of Ag/*p*-Si, Al/$SiO_2$/*p*-Si Schottky barrier diodes, Al/tetraamide-I/*p*-Si diode, Ag/Zn(Phen)q/*p*-Si diode, Ag/FSS/*p*-Si diode [25–29]. The obtained barrier height (0.76 eV) of the Al/*p*-Si/$SiO_2$/DNA/Ag is lower than that of Al/*p*-Si/$SiO_2$/Ag diode (0.82 eV), whereas it is higher than that of *p*-Si/DNA diode (0.56 eV) [20]. This suggests that the DNA organic layer modifies the barrier height and DNA layer gives an excess barrier. The studies in literature have shown that effective Schottky barrier could be either increased or decreased by using organic thin layer on inorganic semiconductor [30–34].

The decrease in the barrier height can result from the realignments between the lowest unoccupied molecular orbital (LUMO), highest occupied molecular orbital (HOMO) of the DNA layer and work function of the metal. The surface modification of DNA layer leads to the changes in the electronic properties of the metal–semiconductor devices due to the molecular tunability of metal/semiconductor diodes.

### *3.2. Interface state density properties*

Figure 3 shows the capacitance–voltage $C$–$V$ plots of Al/*p*-Si/$SiO_2$/Ag [20] and Al/*p*-Si/$SiO_2$/DNA/Ag diodes under various frequencies. It is seen that the capacitance at positive voltages remains to tend constant, but at negative voltages, the capacitance increases with decreasing frequency. The $C$–$V$ plots of the diodes indicate a *p*-type behavior. The change in the capacitance with the voltage is due to the change of width of depletion layer with the applied voltage. As seen in $C$–$V$ plots, the plots have a peak and the intensity and position changes with the frequency. It is evaluated that the peak is distributed with series resistance. Thus, we have corrected the capacitance and conductance plots of the diodes by the following relations [35, 36]:

$$C_{adj} = \frac{\left[G_m^2 + (\omega C_m)^2\right] C_m}{a^2 + (\omega C_m)^2} \tag{3}$$

with

$$a = G_m - \left[G_m^2 + (\omega C_m)^2\right] R_s, \tag{4}$$

where $C_{adj}$ is the corrected capacitance, $G_m$ and $C_m$ are the measured conductance and capacitance, respectively, $\omega$ is the angular frequency.

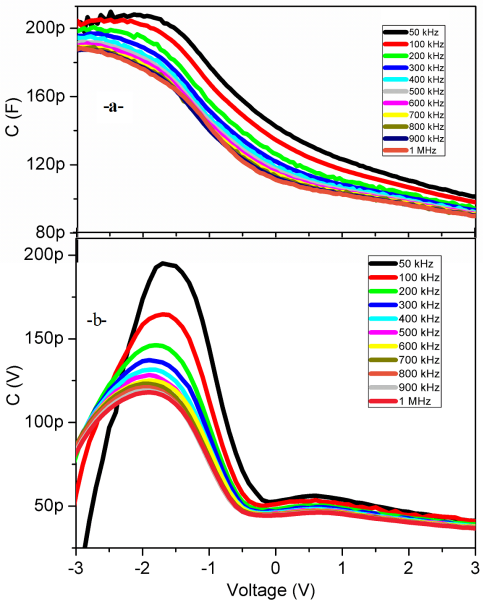


Fig. 3. $C$–$V$ plots of the diodes under various frequencies: (a) Al/*p*-Si/$SiO_2$/Ag [20], (b) Al/*p*-Si/$SiO_2$/DNA/Ag.

Figure 4 shows the plots of $C_{adj}$ vs. $V$ of the Al/*p*-Si/$SiO_2$/Ag [20] and Al/*p*-Si/$SiO_2$/DNA/Ag diodes under various frequencies. It is seen in $C_{adj}$ plots that the curves indicates a symmetric peak. The presence of the peak is due to the presence of interface charges. The

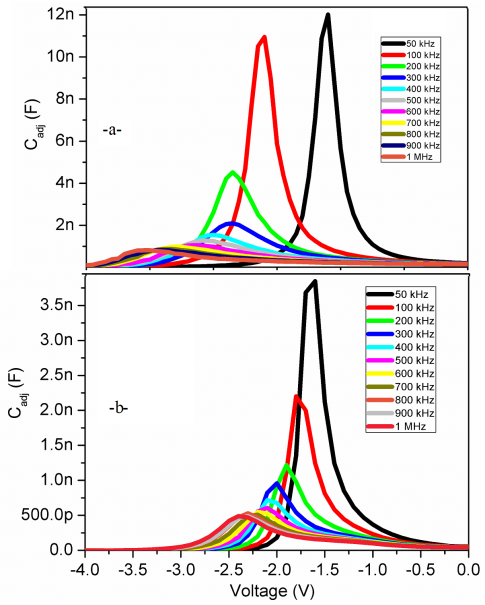


Fig. 4. $C_{adj}$–$V$ plots of the diodes under various frequencies: (a) Al/$p$-Si/$SiO_2$/Ag [20], (b) Al/$p$-Si/$SiO_2$/DNA/Ag.

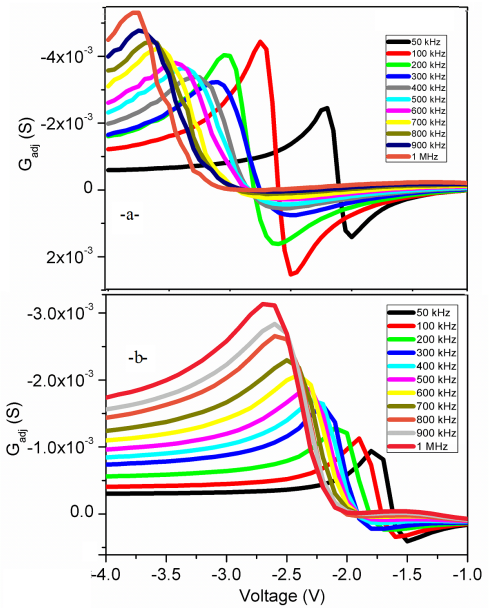


Fig. 5. Plots of $C_{adj}$–$V$ of the diodes under various frequencies: (a) Al/$p$-Si/$SiO_2$/Ag [20], (b) Al/$p$-Si/$SiO_2$/DNA/Ag.

peak intensity decreases with increasing frequency. The conductance–voltage plots of the diodes were corrected by the following relation [35, 36]:

$$G_{adj} = \frac{\left[G_m^2 + (\omega C_m)^2\right] a}{a^2 + (\omega C_m)^2}, \tag{5}$$

where $G_{adj}$ is the corrected conductance.

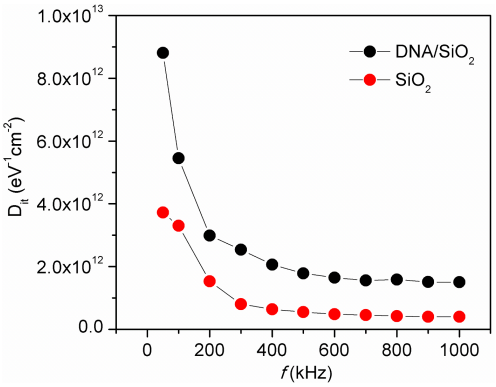


Fig. 6. Plots of $D_{it}$ vs. $f$ for the diodes.

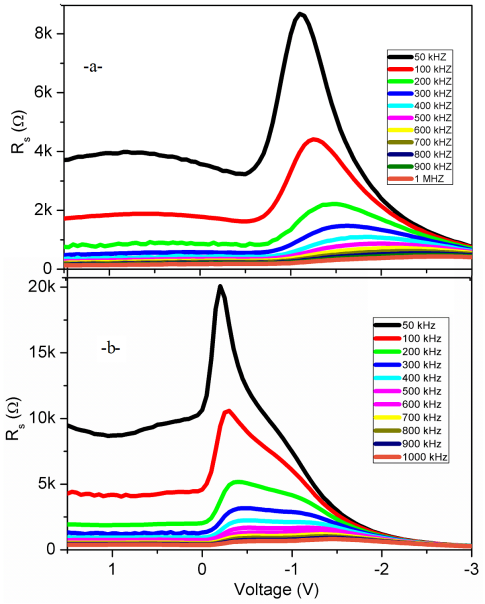


Fig. 7. Plots of $R_s$–$V$ of the diodes under various frequencies: (a) Al/$p$-Si/$SiO_2$/Ag [20], (b) Al/$p$-Si/$SiO_2$/DNA/Ag.

The obtained plots of $G_{adj}$ vs. $V$ under various frequencies are shown in Fig. 5. The peak in the plots shifts to the negative voltages and peak position increases with frequency. The change in peak height shows that the interface charges follow the frequency. The density of interface states of the diodes was determined by the following formula [37]:

$$D_{it} = \frac{2}{qA} \frac{G_{max}/\omega}{(G_{max}/\omega C_{ox})^2 + (1 - C_m/C_{ox})^2}, \tag{6}$$

where $C_m$ is the measured capacitance, $G_{max}$ is the measured maximum conductance, $\omega$ is the angular frequency, $C_{ox}$ is the capacitance of the insulator layer, $A$ is the area of the diode and $\omega$ is the angular frequency.

Figure 6 shows the plots of $D_{it}$ vs. $f$ for the Al/$p$-Si/$SiO_2$/Ag [20] and Al/$p$-Si/$SiO_2$/DNA/Ag diodes. The $D_{it}$ values are decreased with frequency. This indicates

that the interface charges follow the frequency of applied voltage. The width of peak in the $C_{\mathrm{adj}}$–$V$ curves with frequency is related to the number of trapped carrier charges at interface. The $D_{\mathrm{it}}$ values of the Al/$p$-Si/$SiO_2$/DNA/Ag are higher than that of Al/$p$-Si/$SiO_2$/Ag junction [20]. This indicates that the DNA layer changes the interface states of Al/$p$-Si/$SiO_2$/Ag junction.

The series resistance plots of the diodes are shown in Fig. 7. As seen in Fig. 7, the series resistance changes with frequency and indicates a peak. The intensity and position of the peak change with the frequency. The intensity of the peak decreases and disappears. The peak intensity for Al/$p$-Si/$SiO_2$/DNA/Ag diode is higher than that of Al/$p$-Si/$SiO_2$/Ag junction. This indicates that Al/$p$-Si/$SiO_2$/DNA/Ag diode has the higher $D_{\mathrm{it}}$ values than Al/$p$-Si/$SiO_2$/Ag junction.

## 4. Conclusions

We have fabricated Al/$p$-Si/$SiO_2$/DNA/Ag and Al/$p$-Si/$SiO_2$/Ag junctions. The electrical performances of the diodes were determined by $I$–$V$ and $G$–$C$–$V$ measurements. The junctions exhibit a good rectifying behavior and the rectifying behavior of the Al/$p$-Si/$SiO_2$/Ag diode changes with DNA modification. The diodes indicate a metal–insulator–semiconductor structure. It was found that the $D_{\mathrm{it}}$ values of the Al/$p$-Si/$SiO_2$/DNA/Ag are higher than that of Al/$p$-Si/$SiO_2$/Ag junction. This indicates that the DNA layer increases the interface states of the conventional Si based on MS contacts.

## Acknowledgments

The present study is a result of an international collaboration program between University of Tabuk, Tabuk, Saudi Arabia and Firat University, Elazig, Turkey. The authors gratefully acknowledge the financial support from the University of Tabuk, project no. 4/1433.

## References

[1] T. Maeda, S. Takagi, T. Ohnishi, M. Lippmaa, *Mater. Sci. Semicond. Process.* **9**, 706 (2006).

[2] M. Shah, M.H. Sayyad, Kh.S. Karimov, M.M. Tahir, *Physica B* **405**, 1188 (2010).

[3] M. Shah, M.H. Sayyad, Kh.S. Karimov, M.M. Tahir, *Optoelectr. Adv. Mater. — Rapid Comm. (OAM-RC)* **3**, 831 (2009).

[4] F. Yakuphanoglu, *Synth. Met.* **158**, 108 (2008).

[5] S. Aydogan, Ü. Incekara, A.R. Deniz, A. Türüt, *Microelectron. Eng.* **87**, 2525i (2010).

[6] J.S. Park, B.R. Lee, J.M. Lee, J.S. Kim, S.O. Kim, M.H. Song, *Appl. Phys. Lett.* **96**, 243306 (2010).

[7] S. Aydogan, K. Çinar, H. Asil, C. Coskun, A. Türüt, *J. Alloys Comp.* **476**, 913 (2009).

[8] P. Hanselaer, W.H. Laflére, R.L. Van Meirhaeghe, F. Cardon, *Appl. Phys. A* **39**, 129 (1986).

[9] R.L. Van Meirhaeghe, W.H. Laflére, F. Cardon, *J. Appl. Phys.* **76**, 403 (1994).

[10] P. Hanselaer, W.H. Laflére, R.L. Van Meirhaeghe, F. Cardon, *Appl. Phys.* **56**, 2309 (1984).

[11] Ş. Aydoğan, M. Sağlam, A. Türüt, *Vacuum* **77**, 269 (2005).

[12] V. Kazukauskas, M. Pranaitis, A. Arlauskas, O. Krupka, F. Kajzar, Z. Essaidi, B. Sahraoui, *Opt. Mater.* **32**, 1629 (2010).

[13] R.K. Gupta, V. Saraf, *Curr. Appl. Phys.* **9**, S149 (2009).

[14] S. Okur, F. Yakuphanoglu, M. Ozsoz, P. Kara Kadayifcilar, *Microelectron. Eng.* **86**, 2305 (2009).

[15] O. Gullu, A. Turut, *J. Alloys Comp.* **509**, 571 (2011).

[16] O. Gullu, *Microelectron. Eng.* **87**, 648 (2010).

[17] L. Cai, H. Tabata, T. Kawai, *Appl. Phys. Lett.* **77**, 3105 (2000).

[18] A.Y. Kasumov, M. Kociak, S. Gueron, B. Reulet, V.T. Volkov, D.V. Klinov, H. Bouchiat, *Science* **291**, 280 (2001).

[19] A.J. Storm, J. Van Noort, S. de Vries, C. Dekker, *Appl. Phys. Lett.* **79**, 3881 (2001).

[20] R.K. Gupta, F. Yakuphanoglu, H. Hasar, A.A. al-Khedhairy, *Synthetic Met.* **161**, 2011 (2011).

[21] G. Muyzer, E. De Waal, A.G. Uitterlinden, *Appl. Environmen. Microbiol.* **59**, 695 (1993).

[22] E.H. Rhoderick, *Metal–Semiconductor Contacts*, Oxford University Press, Oxford 1978.

[23] Y. Selzer, A. Salomon, D. Cahen, *J. Phys. Chem. B* **106**, 10432 (2002).

[24] Y.J. Liu, H.Z. Yu, *Chem. Phys. Chem.* **3**, 799 (2002).

[25] S. Acar, S. Karadeniz, N. Tuğluoğlu, A.B. Selçuk, M. Kasap, *Appl. Surf. Sci.* **233**, 373 (2004).

[26] A. Tataroğlu, Ş. Altındal, M.M. Bülbül, *Nucl. Instrum. Methods Phys. Res. A* **568**, 863 (2006).

[27] T. Kılıcoglu, M.E. Aydın, G. Topal, M.A. Ebeoglu, H. Saygılı, *Synthetic Met.* **157**, 540 (2007).

[28] F. Yakuphanoglu, B.J. Lee, *Physica B* **390**, 151 (2007).

[29] M.E. Aydina, F. Yakuphanoglu, *J. Phys. Chem. Solids* **68**, 1770 (2007).

[30] F. Yakuphanoglu, B.-J. Lee, *Physica B* **390**, 151 (2007).

[31] M.E. Aydin, F. Yakuphanoglu, Jae-Hoon Eom, Do-Hoon Hwang, *Physica B* **387**, 306 (2007).

[32] M. Çakar, N. Yıldırım, H. Doğan, A. Türüt, *Appl. Surf. Sci.* **252**, 2209 (2006).

[33] Ş. Aydoğan, M. Sağlam, A. Türüt, *Polymer* **46**, 10982 (2005).

[34] I.H. Campbell, S. Rubin, T.A. Zawodzinski, J.D. Kress, R.L. Martin, D.L. Smith, N.N. Barashkov, J.P. Ferraris, *Phys. Rev. B* **54**, 14321 (1996).

[35] E.H. Nicollian, A. Goetzberger, *Bell Syst. Technol. J.* **46**, 1055 (1967).

[36] I. Dökme, Ş. Altındal, T. Tunç, I. Uslu, *Microelectron. Reliab.* **50**, 39 (2010).

[37] W.A. Hill, C.C. Coleman, *Solid State Electron.* **23**, 987 (1980).